International Journal of GEOMATE, May., 2021, Vol.20, Issue 81, pp.132-145
ISSN: 2186-2982 (P), 2186-2990 (O), Japan, DOI: https://doi.org/10.21660/2021.81.GX254
Geotechnique, Construction Materials and Environment

PROPERTIES OF GRANULATED BENTONITE MIXTURES FOR RADIOACTIVE WASTE DISPOSAL: A REVIEW

*Mazhar Nazir [1], Ken Kawamoto [1], and Toshihiro Sakaki [2,3]

[1]Graduate School of Science and Engineering, Saitama University, Japan
[2]Department of Civil and Earth Resources Engineering, Kyoto University, Japan
[3]Now at Environmental Science and Engineering Consulting, Japan

* Corresponding Author, Received: 15 Jun. 2020, Revised: 30 Jan. 2021, Accepted: 13 Feb. 2021

ABSTRACT: Bentonite has long been considered as a potential sealing material in engineered barrier systems (EBS) for the geological disposal of radioactive waste due to its favorable physical and chemical properties. In some disposal concepts, the research evolution has led to the adaption of granulated bentonite mixtures (GBM) as a candidate buffer/backfill material owing to its high compaction properties, operational advantages, and ability to close gaps between the seal and host rock. A thorough understanding of the behavior of GBM is essential for proper design and construction of an efficient repository. As compared to compacted bentonite blocks, studies on GBM are somewhat limited. Thus, a review of former experimental studies conducted on GBM over the past two decades was performed. The topics included compaction properties, thermo-hydro-mechanical properties, gas transport, and microstructure. This work comprises a summary table listing material properties, sample scale, methodology, test conditions, and graphical representation of results. Based on the review, prospects for further investigations/studies have also been recommended to understand the behavior of GBM.

Keywords: Granulated bentonite mixtures (GBM), Radioactive waste disposal, Buffer/backfill material, Dry density, Thermo-hydro-mechanical (THM) properties

1. INTRODUCTION

In countries where deep geological disposal of nuclear waste is being considered, various repository design concepts have been studied over the last four decades [1]. These include encapsulation of nuclear waste in metal canisters placed in vertical holes or horizontal tunnels constructed in deep geological formations [1,2]. The space between the metallic canisters and the hole or tunnel is to be filled with a buffer material, and the other part of the tunnel is to be sealed with backfilling material(s). Owing to its favorable physical and chemical properties, bentonite has been extensively studied as a backfilling/buffer material in radioactive waste disposal concepts [3]. These properties include low permeability and high water retention capacities [4,5], high swelling capacity [3,5], thermal characteristics [3], and microporous structure [5].

Many design concepts consider pre-compacted blocks of bentonite as a buffer material, e.g., the prototype repository in-situ test carried out at the Äspö Hard Rock Laboratory in Sweden [4]. Alternatively, granulated bentonite mixtures (GBM) consisting of granules (highly compressed pellets) and powders in a mix of graded proportions have also been considered as the buffer material [6] as adopted by National Cooperative for the Disposal of Radioactive Waste (NAGRA) in the prototype Full-scale Emplacement (FE) experiment [7] and Engineered Barrier (EB) experiment [8,9] at Mont Terri rock laboratory in Switzerland. GBM is purported to improve emplacement operations including ease of transportation and in-situ placement/backfilling, achieve good compaction attributes to meet a required emplacement dry density. Additionally, GBM is considered to have high adaptability to irregular rock wall conditions [10]. With this application, bentonite pellets have also been used as a gap-filling material to fill the voids between bentonite blocks and host rock [4].

In a typical repository environment, a GBM barrier will be subjected to the radiogenic heat of the waste canister and hydration due to groundwater from the surrounding rock. The buffer of GBM should be able to rapidly dissipate radiogenic heat and maintain its low water permeability, as well as develop sufficiently high swelling pressure to maintain good contact between the host rock and waste. Various gases are also generated by metal corrosion or degradation of organic wastes. The GBM buffer should be permeable enough to allow the transport of gases without cracking or rupturing of the buffer due to excessive gas pressures [3]. Owing to the complexity of the problem and functional requirements of buffer, an accurate assessment of thermo-hydro-mechanical (THM) properties and

gas transport processes is essential to design and implement an efficient and a safe barrier. Till now various studies have been conducted to understand the performance of GBM. This paper summarizes the key findings of experimental studies performed in the last couple of decades with a special focus on compaction, hydraulic, thermal, and gas transport properties as well as the microstructure.

2. METHODOLOGY

A literature search was carried out using search engine Google Scholar and Web of Science™ (Clarivate Analytics) with several key words including bentonite, granulated bentonite mixtures (GBM), bentonite pellet mixtures, buffer, backfill, engineered barrier, radioactive/nuclear waste disposal and geological disposal/repositories. Among many studies on THM properties of bentonite, the majority were on compacted forms or blocks, and the target materials of this review were GBM and pellet mixtures. The granulated materials are different from compacted blocks in the sense that their dry densities can be lower and pore sizes can be larger. Based on this search process, the papers and reports related to THM and gas transport studies published mainly after 2000 were selected for review and comparison. The present review comprises summary tables listing materials and methodology, test conditions, and graphical representation of results.

3. GRANULATED BENTONITE MIXTURES (GBM)

For engineered barriers in repositories, various kinds of bentonites have been selected and are being considered worldwide. The GBM and pellet mixtures presented in this review comprise several bentonite materials, mainly MX-80, Serrata, Kunigel (V1 and GX), FoCa, and GMZ. MX-80 GBM from Wyoming, USA, is a sodium montmorillonite bentonite and was adopted by NAGRA in the FE experiment [7]. Serrata GBM produced from bentonite deposits (the same origin as FEBEX bentonite) in the zone of Serrata (Almería, Spain) was used in the EB experiment at the Mont Terri rock laboratory [8].

Kunigel V1 [11] and Kunigel GX [12] are bentonites from Japan that have been studied as a potential barrier material for a high-level radioactive waste (HLW) disposal concept in Japan. As a part of a prototype repository project in 2002, Sugita [13] examined Kunigel V1 pellets as a material to fill the gaps between bentonite blocks and rock mass. Recently, Kunigel GBM was used to fill the voids between the prefabricated engineered barrier system module (PEM) and tunnel wall at Horonobe Underground Research Laboratory (URL), in Hokkaido, Japan [14]. The pellets and pellet/powder mixtures of two other bentonite materials, FoCa (France) and GMZ (China), have been used as either buffer or gap-filling materials in the RESEAL project [4] and mock-up tests in China [15], respectively. The basic properties of these materials are presented in Table 1 [16].

4. COMPACTION PROPERTIES

The emplaced dry density (DD) is an important design parameter that controls the effectiveness of a buffer/backfill. Various factors affect the DD of an emplaced sealing material, including particle shape, density of the individual particles (a single pellet or granule), particle size distribution, and the method of emplacement. High DD values can be achieved by using the particle size distribution corresponding to the Fuller curve [17]. NAGRA conducted a series of laboratory tests to evaluate the effects of particle sizes and particle size distributions. Various grain size mixtures of MX–80 pellets ranging in size from 0–16, 0–10, 0.63–10, and 0–24 mm (all follow the Fuller curve) and 10–16 mm (narrow size range) were emplaced in simulated boreholes (transparent pipes) in vertical and horizontal orientations. The results indicated that GBM matching the Fuller curve yielded higher DD values than the narrow particle size distributions of 10–16 mm. Additionally, matching the particle size distribution to the Fuller curve proved to be an effective method to achieve DD values greater than 1.5 g/cm^3 [18].

Table 1. Basic properties of bentonite materials [13]

Material	Type of Bentonite	Mineral Density (g/cm^3)	Montmorillonite (%)	LL (%)	PL (%)	PI	CEC (meq/100 g)	SSA (m^2/g)
MX80	Na	2.76	79	519	35	484	82.3	522
Serrata	Ca	2.70	92±3	102	53	49	102	725
Kunigel V1	Na	2.79	46–49	474	27	447	73.2	687
FoCa	Ca	2.67	80*	112	50	62	54	300
GMZ	Na	2.66	75.4	313	38	275	77.3	570

LL: Liquid limit, PL: Plastic limit, PI: Plasticity index, CEC: Cation exchange capacity, SSA: Total specific surface area,
* Interstratified smectite/kaolinite

The compaction properties of seven types of bentonite ores with different physicochemical properties were studied using four granular bentonites from Japan (mined at the Tsukinuno mine in Yamagata Prefecture) and three granular bentonite ores from Wyoming, USA. Three different particle size distributions were prepared for each bentonite ore, with the grain sizes of <10 mm, <2 mm, and 1.6–10 mm. The grain size distribution curves for granular bentonites of <10 mm size are shown in Fig. 1. The water contents (w.c.) of all bentonite ores ranged between 15–20%. Compaction tests were carried out on these various particle size ranges and resulting compaction characteristics curves (DD vs. w.c.) were prepared.

The findings indicated that the compaction characteristics were more strongly affected by the kind of bentonite ore (bentonite ore properties) than the particle size range. A correlation was developed to calculate the maximum dry density and optimum water content of granular bentonite from the plastic limit of powdered bentonite ore. In addition, the calculations and cross-sectional observations showed that the homogenization process of finer fractions in the void spaces between the coarser fractions (load bearing grains) was also a controlling factor for the compaction process of granular bentonite [19].

In a more recent study [20], several MX80 GBMs with different grain size distributions similar to the Fuller curve were examined. It was shown that the fraction of fines could be an important factor to achieve higher compaction dry density. The best mixture was used in the FE experiment at the Mont Terri rock laboratory [7] where the target DD of 1.45 g/cm^3 was achieved.

5. THERMAL PROPERTIES

The thermal properties, such as thermal conductivity and heat capacity, are the main parameters that govern the heat transfer characteristics of bentonite buffers. The thermal conductivity of a buffer refers to how effectively the radiogenic heat of the canister can be transported through the buffer to surrounding rock. Information on volumetric heat capacity is required to accurately calculate the time-dependent temperature field around the metallic canister [21]. The thermal characteristics of the porous medium are governed by various factors including composition, grain and pore size structure, dry density [22], porosity [22,23], moisture content [23,24], and temperature [24]. The thermal properties of various GBM and pellet mixtures were measured in the laboratory by different methods. Table 2 provides a summary of details of the tested materials and methodology. It is noted that the majority of existing research on the thermal properties of GBM focused on thermal conductivity, and information on heat capacity was limited.

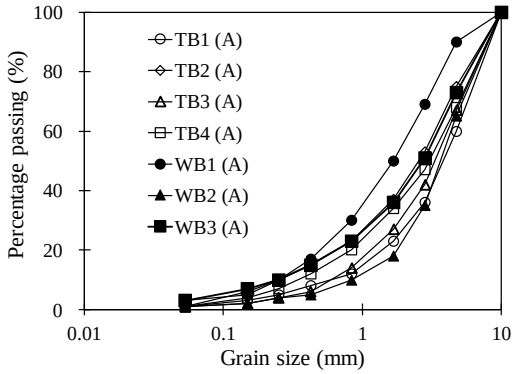

Fig. 1 Grain size distribution curves of granular bentonites (less than 10 mm size) [19].

5.1 Thermal conductivity

5.1.1 Effect of dry density

The solid phase (GBM particles) is more thermally conductive than the air in the voids. For a fixed water content, the existing results generally indicate that thermal conductivity increases with increasing dry density, Fig. 2(a) [13,24-29]. Uniformly graded pellet mixtures yielded low thermal conductivities despite having higher water contents. The reason may be attributed to higher porosity due to the larger voids/gaps between the pellets. This emphasizes the necessity of adding fines to pellet mixtures, thereby filling the voids between the pellets and creating an interconnected homogeneous mixture of fine and coarse pellets, which will result in higher thermal conductivities.

5.1.2 Effect of moisture content

The moisture-dependent thermal conductivity of GBM is presented in Fig. 2(b) [13,24,27,29]. The thermal conductivity is strongly dependent on the moisture content. Liquid water in the pores functions as a thermal bridge between solid particles [30,31]. Its behavior is, however, different for different material conditions. Even for the same MX80, GBM and pellets resulted in quite different behaviors largely due to the porosity differences described above.

MX80 GBM was used in a full-scale in-situ demonstration experiment as buffer around the heaters mimicking waste in an FE experiment [7]. The authors measured a gradual increase of thermal conductivities over a period of one year after the emplacement of GBM, indicating a slow wetting of GBM due to water inflow at a very low

Table 2: Summary of materials and methodology adopted for determination of thermal properties

Material	w.c. (%)	Pellet DD (g/cm^3)	Gradation (mm)	Apparatus/Methodology	Target Parameter	Ref
MX80 GBM	-	2.18	0.1–9.5	Field measurements by 10 cm long single needle heat pulse sensors from full scale project	T.C. vs. w.c.	[7]
Kunigel V1	9.5	1.91	Pellet: 11×7.4	Cylindrical shape pellets (5×3cm) filled at DD=1.0 g/cm^3, hot disc method, double spiral sensor sheet	T.C. vs. DD/w.c.	[13]
MX80 GBM	4.5 5.9	2	0.065–6.5	Double spiral heating sensor (thin metal sheet insulated by a Kapton body) was used for measurements. For the w.c. and T series, the DD ranged around 1.6 and 1.7 g/cm^3. Measurements at varying T between 25 to 105 ºC	T.C. vs. DD, w.c./T, S.H.C. vs. T/w.c.	[24]
MX80 GBM	5.5	2.18	0.1–6.3 with fines	Sample size=6×15cm. KD2 Pro thermal analyzer TR-1 probe	T.C. vs. DD	[25]
GBM	7.5	1.7-1.96	0.075–19	Various types of bentonite pellets were filled at the target DD	T.C. vs. DD	[26]
MX80	16.6	–	Pellet: 12×12×6	Pillow-shaped pellets filled in mould (119×119×31cm) at target DD 1.075 g/cm^3. A Hot-Box device used for measuring thermal conductivity	T.C. vs. DD/w.c.	[27]
MX-80	16	–	Pellet: 12×12×6	Sample size=15×20cm. Thermal probe (16 cm long), pellets filling at DD=1.045 g/cm^3	T.C. vs. DD	[28]
MX-80	16	–		Roller-compacted sample (45x45x8cm). Heat flow meter method, pellets hand compacted into insulated frame at DD=1.26 g/cm^3, frame inserted in hot-box machine	T.C. vs. DD	[28]
MX-80	17.4 11.9	–	< 2	Compacted samples (5×7cm) of two granular bentonites (with different quartz content), heating wire probe thermal analyzer	T.C. vs. DD/w.c.	[29]

DD: Dry density, w.c.: Water content, T.C.: Thermal conductivity, S.H.C.: Specific heat capacity, T: Temperature

rate from the tunnel wall. It was further observed that the rate of thermal increase was higher at points located close to local water inflow spots (e.g., near rock bolts).

5.1.3 Effect of temperature

Wieczorek [24] investigated the effect of temperature on the thermal conductivity of GBM. Two sets of samples, at natural water contents (4.5–5.9%) and after oven-drying at 105°C, were prepared in the laboratory. As shown in Fig. 2(c), the thermal conductivity of the samples with natural water content increased with increasing temperature from a value 0.34 W/m/K at 25°C to 0.44 W/m/K at 105°C. A possible explanation for this increase may be that an additional heat transfer takes place in the form of latent heat due to evaporation and condensation between the water pockets at elevated temperatures [32]. During these experiments, the measured thermal conductivities for moist and dried GBM samples at six temperatures matched well. Surprisingly, the dried samples had higher thermal conductivities than those of moist samples. The authors reported the discrepancy was caused by a coupling problem of the measuring probe and granular samples, and the problem was more pronounced in dry samples.

The effects of temperature on compacted bentonite specimens have been previously studied by various researchers. For the compacted MX-80 powdered bentonite, Knutsson [21] showed an increment of thermal conductivities of 3–8.5% in the temperature range from 50° to 90°C. Similarly, Beziat [33] reported that thermal conductivities of calcic smectite samples (DD=1.99 g/cm^3) increased 10% with the increase of temperature from 50° to 188°C. The recent works on GBM conform to previous studies on the compacted bentonites; however, further studies are needed due to limited data.

5.1.4 Effect of mineralogy

The thermal conductivity of soil solids depends on minerals composition. As there are no

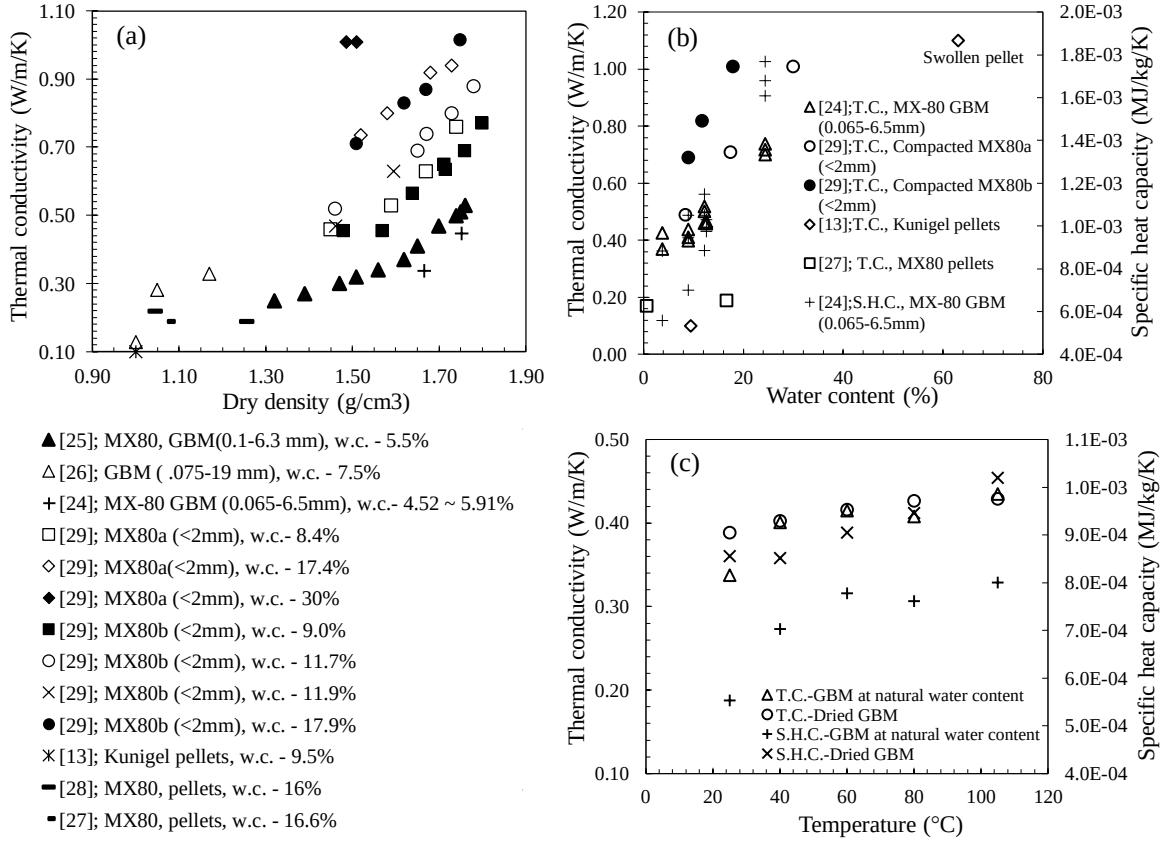

Fig. 2 Variation of thermal conductivity (T.C.) and specific heat capacity (S.H.C); T.C. with dry density (a), water content (b) and temperature (c)[24]; S.H.C with water content (b) and temperature (c) [24].

significant differences in the thermal conductivity of smectites, the major changes in the thermal conductivity of the solids result from the quantity and type of accessory minerals, and additives, e.g. the proportions of quartz and graphite, increase thermal conductivities [30]. Tang [29] measured thermal conductivities of two compacted MX-80 bentonites with different quartz contents at the same water contents and showed that thermal conductivities increased with increasing quartz content.

5.2 Specific heat capacity

The moisture-dependent specific heat capacity behavior is presented in Fig. 2(b) [24]. The specific heat capacity (or, mass heat capacity) also showed a significant dependence on moisture content suggesting that the specific heat of water is an important factor for moist GBM. Similarly, the temperature-dependent specific heat capacity behavior can be observed in Fig. 2(c) [24].

6. HYDRAULIC PROPERTIES

Among various features, an important function of a buffer is to limit water flow through the repository, thereby reducing the potential for corrosion, waste dissolution, and release of radionuclides. Immediately after closure of the repository, the granular buffer material is unsaturated, i.e., water and air coexist in the voids of the buffer [34], giving the bentonite buffers a high suction. Then, along with the continuous water infiltration from the host rock, the bentonite barrier becomes saturated. Thus, the saturation kinetics of a bentonite buffer is one of the features that requires more attention to predict accurately the long-term hydraulic behavior. The hydraulic conductivity and water retention characteristics are key properties to determine the hydraulic behavior of the barrier [35].

The water retention characteristics and hydraulic conductivity of GBM and pellet mixtures were examined in the laboratory by various researchers [8,9,12,13,15,26,36-39]. The tested materials, methodology, and the experimental conditions are summarized in Table 3.

6.1 Water Retention Characteristics

The water retention curves of Serrata and GMZ pellet mixtures under constant volume conditions

Table 3 Summary of materials and methodologies adopted to determine hydraulic properties

Material	Gradation (mm)	Apparatus/Methodology	Target Parameter	Ref.
Serrata Pellet mixture	0.4–10	Wetting at constant volume, tests at DD=1.3, 1.5, 1.9 g/cm^3. S controlled by vapor transfer (S,300~3MPa) and axis translation technique (S=3 MPa~ zero/sat)	S vs. w.c.	[36]
GMZ Pellet mixture	0.075–7	Sample size=5x3.5cm. Wetting at constant volume, tests conducted at DD=1.45 g/cm^3. S controlled by vapor equilibrium technique (S ≥ 4.2 MPa) and osmotic technique (S < 4.2 MPa)	S vs. w.c.	[15]
Serrata GBM	0.4–10	Constant gradient permeability tests, steady state conditions		[8]
MX80 Pellet	< 10	Small sample holders (3.5×1cm), 20°C, 17 days hydration time, test solution - synthetic water (0.2 mole/L NaCl)		[9]
Kunigel V1	Pellet: 11×7.4	Sample size=5×3cm. Cylindrical-shape pellets filled in the test cell at DD=1.08 g/cm^3, distilled water solution, water injection pressure 0.01 to 0.15 MPa,		[13]
GBM	0.075–19	Different types of bentonite pellets were filled at the target DD		[26]
Kunigel, GX Granular	< 10	Full scale mock-up test, granular bentonite compacted on-site using vibratory rollers to achieve a target dry density 1.50–1.70 g/cm^3 with the w.c. 21.0+2%.	H.C. vs. DD	[12]
GMZ Pellet mixture	0.075–7	Sample size=5×3.5cm. Sample prepared at DD=1.45 g/cm^3, test performed under constant volume conditions by 1000 kPa water pressure.		[15]
Serrata GBM	0.075–10	Large oedometer cell (10×5cm) was used, deionized water		[37]
Serrata P/P (P/P=70/30)		Large oedometer cell (10×10cm) was used, deionized water		
MX80 P/P (P/P=80/20)	Pellet: 32	Oedometer cell (12×6.4cm), Tests at DD=1.41–1.54 g/cm^3 constant volume condition, synthetic water, T=22°C±1°.		[38]
Serrata grains	< 5	Oedometer cell equipped with a silicone oil thermostatic bath, constant volume, deionized water	H.C. vs. T	[39]

DD: Dry density, S: Suction, w.c.: Water content, H.C.: Hydraulic conductivity, T: Temperature, d: Diameter, h: Height, sat: Saturation, P/P: Pellet/Powder

are presented in Fig. 3 [15,36]. At high suction, both materials have comparable water retention properties. On the other hand, the water contents of tested materials varied depending on the packed void ratio at lower suction rates. A possible explanation is that the water retention curve is independent of the void ratio [36] and initial conditions such as DD and fabrics at high suction [15]. Water is stored within the pellets as intra-pellet water, and the water content of the sample is conditioned by material characteristics, including specific surface of clay and the soil microstructure as well as the pore fluid chemistry. Conversely, the water retention curve becomes dependent on the void ratio at lower suction rates, and the water content increases to fill the inter-pellet voids with decreasing suction [36].

6.2 Hydraulic Conductivity

The hydraulic conductivity of a porous medium is affected by various factors including grain size distribution, particle structure, water content (or degree of saturation), density, and void ratio [40]. Figure 4 [8,9,12,13,15,26,37,38] presents the effects of DD on the saturated hydraulic conductivities of GBM and pellet mixtures**.** The plots show that hydraulic conductivities decreased with increasing DD. Villar [39] investigated the effect of temperature on the saturated hydraulic conductivity of compacted Serrata granular bentonite using a thermostatically controlled oedometer cell under a constant volume. The results showed the hydraulic conductivities increased with temperature in the range of 25–80 ºC (Fig. 5). As expected by the authors, the increase of hydraulic conductivities can be attributed to the decreasing kinematic viscosity of water with increasing temperature. Additionally, the effect of temperature on hydraulic conductivities may differ depending on the type of minerals (montmorillonite, kaolinite, and saponite) and the types of cations in the exchange complex [41].

Masuda [26] reported the effects of salinity of groundwater on the saturated hydraulic conductivity of granulated bentonite. The authors showed that salinity had a strong influence on the hydraulic properties; the saline water resulted in higher hydraulic conductivity values than fresh water. The increase in hydraulic conductivity with salinity content may be attributed to three mechanisms: alterations of pore configurations due to the change of swelling pressures, formation

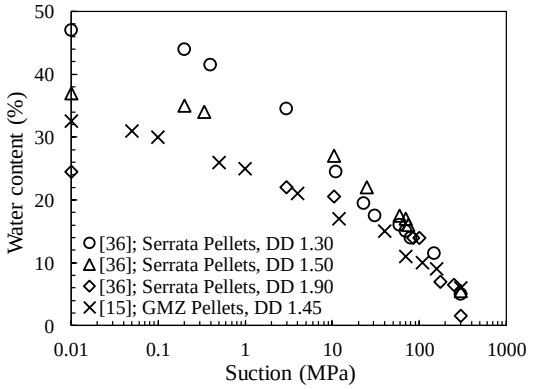

Fig. 3 Water retention curves of the pellet mixtures under constant volume conditions [15,36].

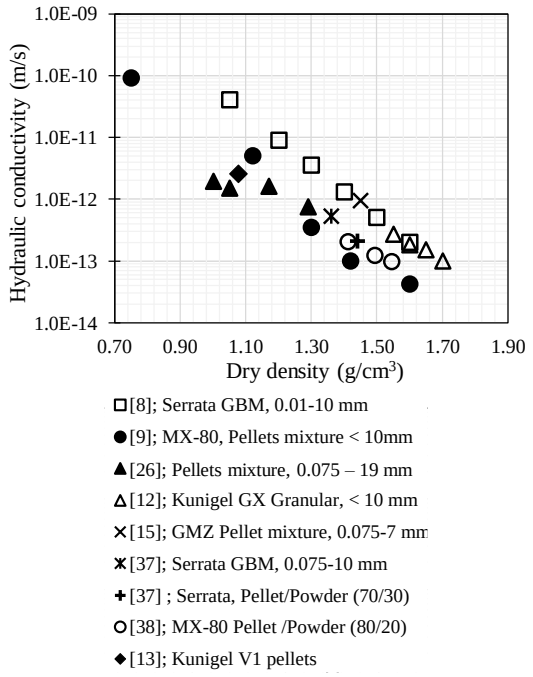

Fig. 4 Effect of dry density on hydraulic conductivity [8,9,12,13,15,26,37,38].

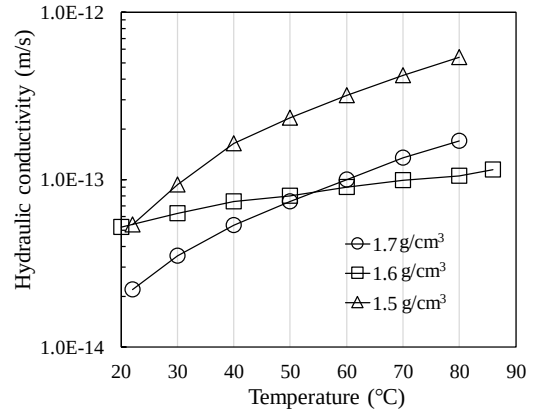

Fig. 5 Effect of temperature on hydraulic conductivity [39].

of diffuse double layers, and variations in the viscous behavior of the water structure. These mechanisms reduce the swelling pressure with increasing saline concentration and increased flow channels that contribute to rapid water flow, resulting in the increase of hydraulic conductivities [30].

7. MECHANICAL PROPERTIES

7.1 Swelling Characteristics

The factors affecting the swelling of the bentonite can be classified into two categories, namely internal factors, including specific surface area, cation exchange capacity, properties of pore water (ion type and concentration), and external factors, such as DD, water content, and compaction method [42]. The maximum swelling pressure increases with increasing montmorillonite content and the initial DD. The maximum swelling strain is more strongly affected by the exchangeable-cation composition in bentonite rather than the montmorillonite content [43].

The swelling characteristics of various GBMs, pellet mixtures, and pellet/powder mixtures have been examined in the laboratory using oedometers/rigid cells under constant volume conditions. Table 4 summarizes the experimental conditions adopted for the swelling pressure testing. The results showed that the swelling pressures increased with increasing DD (Fig. 6) [2,4,8,9,13,37-39,44-51]. In Fig. 6, a non-linear relationship between DD and swelling pressure is evident. It was also observed that FoCa pellet/powder mixtures developed low swelling pressures as compared to MX-80 and Serrata mixtures. This may be attributed to a difference in the mineral properties of FoCa, which has a low smectite content with beidellite and kaolinite in a 50:50 (%) ratio.

The temperature-dependent swelling of compacted Serrata granulated bentonite has been studied in a thermostatically controlled oedometer cell, and the results indicated that the swelling pressure decreased with the increase in temperature (Fig. 7) [39]. These results agreed with the findings of Pusch [52], demonstrating that the swelling pressure of montmorillonite under the temperature variations was governed by a predominant cation in the exchange complex. With the increase of temperature, the swelling pressure increased in sodium-bentonite and decreased in calcium-bentonite. Because Serrata bentonite is predominately a calcium-bentonite (Table 1), the swelling pressure decreased with increasing temperature.

Table 4: Summary of materials and methodology adopted for determination of mechanical characteristics

Material	Gradation (mm)	Major Mineral (%)	Sample size (cm)	Apparatus/Methodology	Target parameter	Ref.
MX80 GBM	0.16-10	85^{sm}	7×48.3	Heated column experiment, test at DD=1.47 g/cm^3, monitored for 3 years	SP vs. DD	[2]
FoCA P/P (P/P = 50/50)	–	$50^{bd}/50^{kao}$	12×5	Constant volume rigid frame cells were used for test. Samples were filled at the target DD between 1.3–1.6 g/cm^3, T=24±1°C		[4]
Serrata GBM	0.01-10	$88\text{-}96^{sm}$	–	Wetting at constant volume conditions		[8]
MX80, GBM	< 10	80^{mon}	3.5×1	Small samples holders, 20°C, 17 days hydration time		[9]
Kunigel V1	Pellet: 11×7.4	–	6×2	49 cylindrical-shape pellets filled in the cell resulting in DD=1 g/cm^3		[13]
Serrata P/P	–	$> 90^{mon}$	10×10	Large oedometer cell, constant volume conditions, DD=1.40 g/cm^3 and 1.45 g/cm^3		[37]
Serrata GBM	0.075–10	$> 90^{mon}$	10×5	Large oedometer cell, constant volume conditions, two experiments at DD 1.35 g/cm^3 (initial water content 4.7% and 8.7%), room temperature		
MX80 P/P (P/P=80/20)	Pellet: 32	80^{sm}	12×6.4	Oedometer cell, constant volume conditions, T - 22 °C, DD varied b/w between 1.20 – 1.59 g/cm^3. Hydration time 230-250 days		[38]
Compacted Serrata grains	< 5	92 ± 3^{mon}	5×1.2	Oedometer cell, constant volume conditions, 30°C	SP vs. DD, T	[39]
MX80 P/P (PP=80/20)	Pellet: 7×7 Powder: < 2	80^{sm}	–	DD=1.49 g/cm^3, constant volume oedometer cell with 70-mm diameter, 440 days hydration time	SP vs. DD	[44]
		80^{sm}	6×12	Constant volume cell, monitored for 160 days, sample prepared at DD=1.49 g/cm^3		[45]
Serrata GBM	0.075–9.5	$> 90^{mon}$	–	In-situ SP measured by sensors in EB experiment, in-situ T, RH (17 °C, 48%)		[46]
FoCA P/P	–	$50^{bd}/50^{kao}$	–	Oedometer tests, samples of 50, 100 and 120 height samples prepared at DD=1.6 g/cm^3, Monitored from 100 days to more than 1 year		[47]
MX80	0.065-4	85^{sm}	7.5×1.5	Constant volume swelling tests in rigid cells		[48]
MX80 shot-clay (Sand 60%, gravel 30%)	–	85^{sm}	7.5×1.9	In-situ cores from shot-clay experiment Grimsel Test Site, constant volume tests in laboratory, maximum swell pressure observed 10 days after the flooding		[49]
MX80 GBM	0.16-10	85^{sm}	–	Testing in large oedometer cells at DD=1.47 g/cm^3, T=23.5±2.6°C, Pearson water (sodium-rich solution of composition similar to Opalinus clay formation, with reported density of 1.020 g/cm^3) was used for experiment. Hydration time 446 days		[50]
MX80 P/P (P/P=80/20)	Pellet : 7×7	80^{sm}	6×12	Infiltration cell, Constant volume conditions, DD=1.49 g/cm^3, monitored for 845 days		[51]
Milos Greece GBM	> 8 (13%) 0.063–8 (87%)	–	6×6	Undrained direct shear tests at a constant shear displacement rate of 0.5 mm/min. Tests conducted at 20% (natural w.c.), 40% and 60% w.c.	SS vs. w.c.	[53]
Milos Greece P/P	Pellet: 4–8 (84%) 0.063–4 (6%)		6×6	Undrained direct shear tests at a constant shear displacement rate of 0.5 mm/min. Tests conducted at 13% (natural w.c.), 20%, 30%, 40% and 60% w.c.	SS vs. w.c.	

DD: Dry density, SP: Swelling pressure, T: Temperature, SS: Shear strength, w.c.: Water content, ^{sm}: Smectite, ^{mon}: Montmorillonite, ^{bd}: Beidellite, ^{kao}: Kaolinite, P/P: Pellet/Powder, RH: Relative humidity

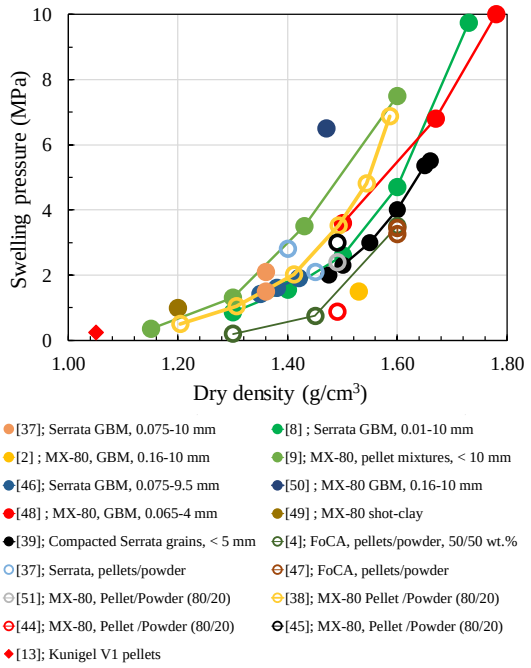

Fig. 6 Swelling pressure as a function of dry density [2,4,8,9,13,37-39,44-51].

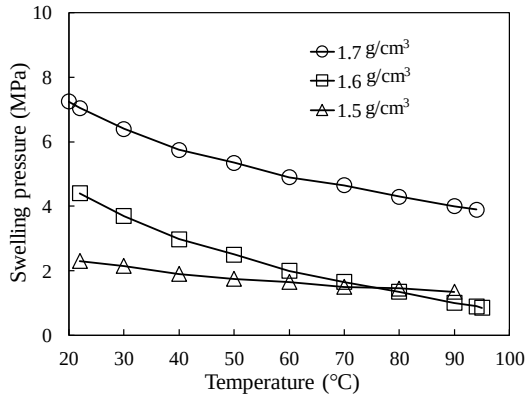

Fig. 7 Swelling pressure as a function of temperature [39].

7.2 Shear Strength

Sinnathamby [53] conducted direct shear tests to examine the shearing behavior of GBM and a pellet powder mixture prepared from the bentonite source, the Isle of Milos, Greece (Material from this source is considered by POSIVA, Finland, in the KBS-3V design concept) (Table 4).

The results indicated that the internal friction angle and cohesion of both materials (GBM and pellet powder mixture) decreased with increasing water content (Fig. 8). GBM exhibited higher shear strength than the pellet powder mixture at water contents >50%. The visual observations revealed that the pellet powder mixture lost its

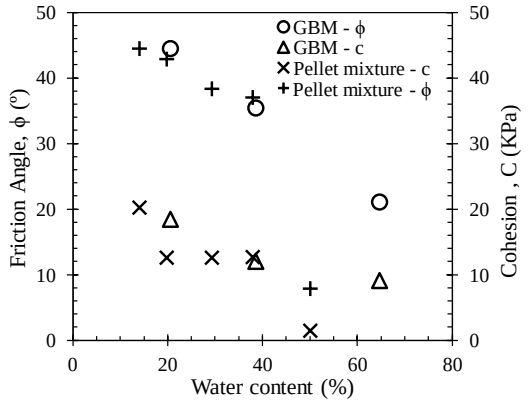

Fig. 8 Shear strength as a function of water content [53].

physical characteristics at water contents >40% and exhibited a gel-like behavior. Conversely, GBM exhibited relatively stable physical characteristics with the increase of water content and showed a gradual loss of shear strength.

8. GAS TRANSPORT

Gas diffusion and advection are the prevailing mechanisms for transport of gases through soil [54,55]. Selin [55] identified diffusion as a dominant transport mechanism for the gas transport through bentonite barriers unless the applied pressure becomes greater than the swelling pressure and back pressure (total stress). Gas transport through a porous medium is affected by various factors, such as particle size distribution, DD, and pore structure parameters including air-filled and total porosity and pore connectivity-tortuosity [54], as well as water content (or degree of saturation). Very limited studies have been conducted to understand gas transport characteristics of GBM and pellet mixtures. Table 5 summarizes the tested materials and methodologies adopted to measure gas transport parameters. Liu [56] measured gas permeabilities of in-situ GBM core specimens (retrieved from dismantling the EB experiment at Mont Terri rock laboratory after 10.5 years of hydration) using argon gas. The GBM was initially emplaced in the EB experiment at DD=1.36 g/cm^3 (w.c. = 4.2%). However, long hydration caused variations in DD values depending on degree of saturation. Higher DD values (>1.36 g/cm^3) were measured from the core specimens retrieved from the locations close to retaining wall/concrete plug. Whereas, the cores specimens from all other sections showed lower DD values (<1.36 g/cm^3). The results indicated that the gas permeabilities decreased with the increase of moisture content (Fig. 9). The measured gas permeabilities were extremely low, on the order of 10^{-22} m^2 at the water content >35%.

Table 5: Summary of materials and methodology adopted for gas transport studies

Material	Gradation (mm)	Apparatus/Methodology	Target Parameter	Ref
Serrata GBM	0.075–10	Gas permeability tests on the GBM specimens retrieved from dismantling of EB experiment at Mont-Terri rock laboratory, triaxial cell apparatus, low confining pressure 0.5–1 MPa, argon gas used as fluid, steady state method.	IGP vs. w.c.	[56]
Serrata grains	< 5	A triaxial cell (sample size: 38×78mm), nitrogen gas as fluid.	GP vs. DD	[57]

IGP: Intrinsic gas permeability, GP: Gas permeability, DD: Dry density, w.c.: Water content

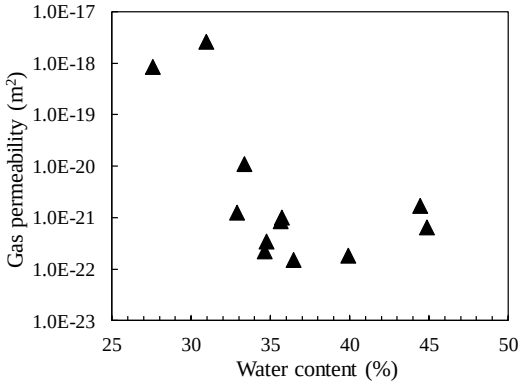

Fig. 9 Intrinsic permeability as a function of water content [56].

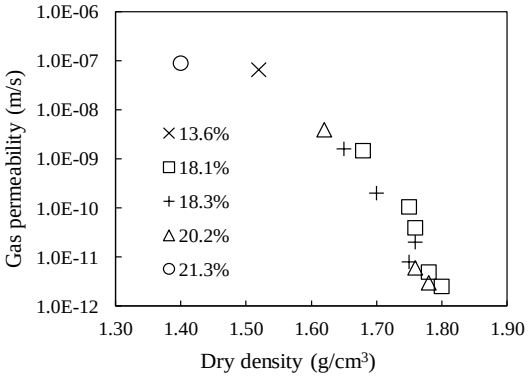

Fig. 10 Average gas permeability as function of dry density for different water contents [57].

Villar [57] measured gas permeabilities of compacted Serrata granular bentonite using nitrogen gas as a fluid and showed that the gas permeabilities decreased with the increase of DD (Fig. 10).

9. MICROSTRUCTURE

Microstructural changes occur in bentonite as a result of compression at the time of emplacement as well as swelling during the hydration process afterwards. Thus, investigations at a microstructural level are crucial to better understand the behavior of bentonite at higher structural levels. Microstructure has been quantitatively examined in terms of pore size distribution (PSD), an important parameter which affects the water, gas, and heat transport properties, adsorption and desorption processes, and structural deformability [58]. Microstructural features/characteristics have been investigated by various methods such as mercury intrusion porosimetry (MIP), scanning electron microscopy (SEM), and microfocus X-ray computed tomography (MFXCT).

As part of the EB experimental program (Mont Terri rock laboratory), Alonso [59] performed MIP tests on Serrata pellet mixtures (uniform pellet fraction of 1–2 mm) to characterize the multiple-porosity network of the samples packed at DD values ranging from 1.15 (achieved by a gravity fall compaction) to 1.95 g/cm^3. A tri-modal PSD curve was obtained in the low-density (1.15 g/cm^3) samples whereas the high-density samples (1.95 g/cm^3) resulted in a bi-modal PSD curve. Comparison of both distributions identified two groups of pores: the first group comprised larger pores classified as inter-pellet voids having a characteristic size around 250 µm and the second group was classified as intra-pellet voids (pores inside and between the clay aggregates contained in a pellet) having a bi-modal distribution with the characteristic sizes at 13 nm and 3 µm. The other measurements at DD = 1.35, 1.45, and 1.7 g/cm^3 changed mainly the macropores (inter-pellet voids), implying that the porosity of inter-pellet voids progressively decreased with increasing DD.

SEM photomicrographs were used to study the sizes of intergranular pores as a function of compaction intensity in the Serrata granular bentonite samples compacted at DD=1.40 and 1.65 g/cm^3; larger intergranular pore sizes were identified in the low-density sample [58]. Structural changes, including fractures and homogenization processes, were investigated by MFXCT during the hydration of pellet and powder mixtures [45]. Nowadays, MFXCT measurements

have been effectively applied in soil science to analyze the pore network structure including pore diameter, pore tortuosity, and coordination [60]. The application of this technique to GBM may lead a better understanding of the pore network structure.

10. FUTURE PROSPECTS

Many research programs are in progress since the 1970s to evolve a safe and sustainable repository for the disposal of high-level radioactive waste, yet no final repository has been constructed [47]. Despite the large number of studies on the bentonite materials used as a buffer/backfill in the repository, some knowledge gaps remain. In-situ experiments with a large focus on GBM are now in progress to understand the coupled effects of complex thermo-hydro-mechanical and chemical processes, e.g., FE [7] and HEE [24] experiments and EB experiment (dismantled [37,56]) at the Mont Terri rock laboratory as well as the new in-situ experiment HotBENT [61] being implemented at the Grimsel Test Site in Switzerland.

Several factors affect the THM properties, gas transport, and microstructural characteristics of GBM. The governing factors identified in this review are summarized in Fig. 11. Some factors, such as DD and grain size distribution, have been comprehensively studied in some cases along with partial work on the moisture content and temperature, whereas other factors such as pore size distribution, and tortuosity are yet to be studied. Therefore, it is recommended that all key factors should be thoroughly examined to further understand the performance of GBM as buffer/backfilling materials.

11. CONCLUSIONS

This paper summarized the key findings of experimental studies conducted on the granulated bentonite mixtures (GBM) apropos their application as buffer/backfill material in the repository design concepts. The review showed that many factors (particle size and density, grain size distribution, dry density, moisture content, porosity, material properties including mineral composition, temperature, and method of compaction/emplacement) greatly affect the compaction, thermo-hydro-mechanical (THM) properties, and gas transport characteristics as well as microstructural behaviors of GBM. Despite the large number of studies, some knowledge gaps still need to be filled to understand the behavior of GBM so that an efficient barrier can be designed and implemented in the future.

It is widely believed that density is a key parameter to ensure the long-term performance of GBM buffer/backfill in a repository because it directly governs the various safety-related aspects. Highly compacted GBM tend to exhibit a block-like behavior resulting into the development of extremely high swelling pressures as well as blockage of the pathways for movement of gases.

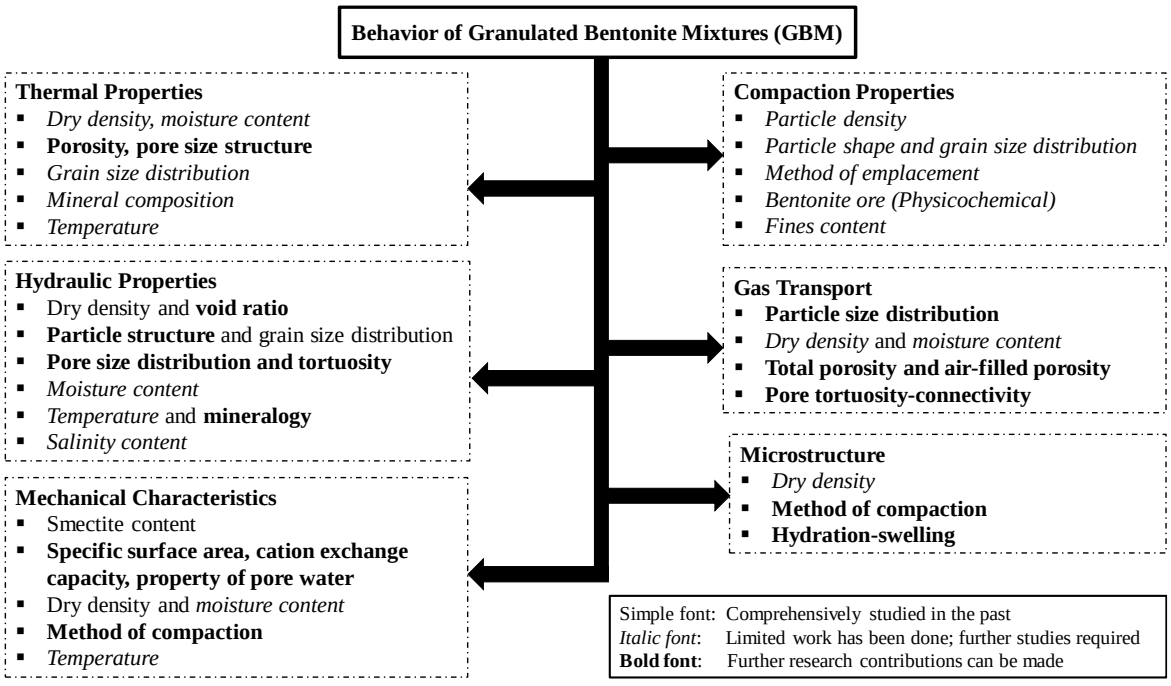

Fig. 11 Factors controlling the behavior of Granulated Bentonite Mixtures (GBM)

Conversely, GBM at low density may exhibit different behaviors, e.g. deficient sealing capacity due to low swelling pressures, besides, it may increase the likelihood of microbial activity (microbially induced corrosion). Therefore, selection of an emplaced optimum dry density of GBM is essential to address all the safety concerns and barrier performance.

12. ACKNOWLEDGMENTS

This work was supported by JSPS KAKENHI Grant Number 17H03301.

13. REFERENCES

[1] Dixon D., Sandén T., Jonsson E. and Hansen J., Backfilling of Deposition Tunnels: Use of Bentonite Pellets, SKB P-11-44, ISSN 1651-4416, February 2011.

[2] Villar M. V., Martín P. L., Romero F. J., Iglesias R. J. and Gutiérrez-Rodrigo V., Saturation of Barrier Materials under Thermal Gradient, Geomechanics for Energy and the Environment, Vol. 8, 2016, pp.38–51.

[3] Arthur R., Sasamoto H. and Yui M., Potential Complications in the Development of a Thermodynamic Database for Hyperalkaline, Argillaceous Systems, Proceedings of the International Workshop on Bentonite-Cement Interaction in Repository Environments, Nuclear Waste Management Organization of Japan (NUMO), October 2004, NUMO-TR-04-05.

[4] Imbert C. and Villar M. V., Hydro-Mechanical Response of a Bentonite Pellets/Powder Mixture upon Infiltration, Applied Clay Science, Vol. 32, Issue 3–4, 2006, pp.197–209.

[5] Wersin P., Johnson L. H. and McKinley I. G., Performance of the Bentonite Barrier at Temperatures Beyond 100 °C: A Critical Review, Physics and Chemistry of the Earth, Vol. 32, Issue 8–14, 2007, pp.780–788.

[6] Volckaert G., Bernier F., Alonso E., Gens A., Samper J., Villar M. V., Martín P.L., Cuevas J., Campos R., Thomas H.R., Imbert C. and Zingarelli V., Thermal-Hydraulic-Mechanical and Geochemical Behavior of the Clay Barrier in Radioactive Waste Repositories (Model Development and Validation), Nuclear Science and Technology. EUR 16744. Commission of the European Communities, Luxembourg, 1996, pp. 722.

[7] Müller H. R., Garitte B., Vogt T., Köhler S., Sakaki T., Weber H., Spillmann T., Hertrich M., Becker J., Giroud N., Cloet V., Diomidis N., and Vietor T., Implementation of the Full-Scale Emplacement (FE) Experiment at the Mont Terri Rock Laboratory, Swiss Journal of Geosciences, Vol. 110, Issue 1, 2017, pp. 287-306.

[8] Mayor J-C., García-Siñeriz J-L., Alonso E., Alheid H-J. and Blümbling, P., Engineered Barrier Emplacement Experiment in Opalinus Clay for the Disposal of Radioactive Waste in Underground Repositories, Technical Report, ENRESA: Empresa Nacional de Residuos Radiactivos, February, 2005, 1–101.

[9] Karnland Q., Nilsson U., Weber H. and Wersin P., Sealing Ability of Wyoming Bentonite Pellets Foreseen as Buffer Material - Laboratory Results, Physics and Chemistry of the Earth, Vol. 33, Issue SUPPL.1, 2008, pp.472–475.

[10] Alonso E.E., Romero E. and Hoffmann C., Hydromechanical Behavior of Compacted Granular Expansive Mixtures, Experimental and Constitutive Study, Géotechnique, Vol. 61, Issue 4, 2011, pp.329–344.

[11] Japan Nuclear Cycle Development Institute (JNC). 2000. H12: Project to Establish the Scientific and Technical Basis for HLW Disposal in Japan, Supporting Report 2, Repository Design and Engineering Technology, JNC TN1410 2000–003, April, 2000.

[12] Yamada A., Akiyama Y., Nakajima M., Yada T., Chijimatsu M., and Nakajima T. (2014). Studies of Construction Methods for Bentonite Engineered Barrier Systems for Sub-Surface Disposal: Vibratory Compaction. Geological Society Special Publication, 400(1), 135–144.

[13] Sugita Y., Suzuki H. and Chijimatsu M., Thermal, Hydrau1ic and Swelling Properties of Bentonite Pellet – Examine on Calculating Parameter Assessment on PRP - (Research Document), JNC TN8400 2002–023, March, 2003.

[14] Radioactive Waste Management Funding and Research Center (RWMC), Summary Report on Research and Development Project on Geological Disposal of High-Level Radioactive Waste in 2016-2020, 2020 (in Japanese).

[15] Liu Z. R., Cui Y. J., Ye W. M., Chen B., Wang, Q. and Chen Y. G., Investigation of the Hydro-Mechanical Behavior of GMZ Bentonite Pellet Mixtures, Acta Geotechnica, Vol. 15, Issue 10, 2020, pp.2865–2875.

[16] Cui Y. J., Tang A. M., Qian L. X., Ye W. M. and Chen B., Thermal-Mechanical Behavior of Compacted GMZ Bentonite, Soils and Foundations, Vol. 51, Issue 6, 2011, pp.1065–1074.

[17] Fuller W. B. and Thompson S. E., The laws of proportioning concrete transaction, American Society of Civil Engineers, 59, 1907, 67 – 143.

[18] Blümling P. and Adams J., Borehole Sealing: Grimsel Test Site Investigation Phase IV, Nagra Technical Report, 07-01, 2008.
[19] Ito H., Compaction Properties of Granular Bentonites, Applied Clay Science, Vol. 31, Issue 1–2, 2006, pp.47–55.
[20] Garitte B., Weber H., and Müller H. R., Requirements, Manufacturing and QC of the Buffer Components Report, LUCOEX – WP2, 2015, 115.
[21] Knutsson S., On the Thermal Conductivity and Thermal Diffusivity of Highly Compacted Bentonite, SKB Report, Swedish Nuclear Fuel and Waste Management Co., SKB, 83–72 October, 1983.
[22] Engelhardt I., Finsterle S., Thermal-Hydraulic Experiments With Bentonite/Crushed Rock Mixtures and Estimation of Effective Parameters by Inverse Modeling, Applied Clay Science, Vol. 23, 2003, pp.111–120.
[23] Côté J. and Konard J. M., Thermal Conductivity of Base-Course Materials, Can. Geotech. J., Vol. 42, 2005, pp.61–78.
[24] Wieczorek K., Czaikowski O. and Miehe R., PEBS, Long-Term Performance of Engineered Barrier Systems, GRS Participation, Report, GRS – 353, December, 2014.
[25] Sakaki T., Firat Lüthi B., Vogt T., Uyama M. and Niunoya S., Heated Fiber-Optic Cables for Distributed Dry Density Measurements of Granulated Bentonite Mixtures: Feasibility Experiments, Geomechanics for Energy and the Environment, Vol. 17, 2019, pp.57–65.
[26] Masuda R., Asano H., Toguri S., Mori T., Shimura T., Matsuda T., Uyama M. and Noda M., Buffer Construction Technique using Granular Bentonite, Journal of Nuclear Science and Technology, Vol. 44, Issue 3, 2007, pp.448–455.
[27] Kivikoski H., Heimonen H. and Hyttinen H., Bentonite Pellet Thermal Conductivity Techniques and Measurements, Working Report 2015-09, POSIVA OY Olkiluoto FI - 27160 EURAJOKI , FINLAND, May, 2015.
[28] Marjavaara P., Holt E. and Sjöblom V., Customized Bentonite Pellets: Manufacturing, Performance and Gap Filling Properties. Working Report 2012-62, December, 2013.
[29] Tang A. M. and Cui Y. J., Determining the Thermal Conductivity of MX-80 Clay, Unsaturated Soils, 2006, pp. 1695-1706.
[30] Villar M. V., Thermo-Hydro-Mechanical Characteristics and Processes in the Clay Barrier of a High Level Radioactive Waste Repository, State of the Art Report, Informes Técnicos Ciemat, 1044, October 2004, p.75.
[31] Smits K. M., Sakaki T., Limsuwat A. and Illangasekare T. H., Thermal Conductivity of Sands under Varying Moisture and Porosity in Drainage–Wetting Cycles, Vadose Zone J., Vol. 9, Issue 1, 2010, p. 172.
[32] Smits K. M., Sakaki T., Howington S. E., Peters J. F. and Illangasekare T. H., Temperature Dependence of Thermal Properties of Sands across a Wide Range of Temperatures (30-70°C), Vadose Zone. J., Vol. 12, Issue 1, 2013, pp.vzj2012.0033.
[33] Beziat A., Dardaine M. and Gabis V., Effect of Compaction Pressure and Water Content on The Thermal Conductivity of Some Natural Clays, Clays and Clay Minerals Vol. 36, No. 5, 1988, pp.462-466.
[34] Villar M.V. and Lloret A., Influence of Dry Density and Water Content on the Swelling of a Compacted Bentonite, Applied Clay Science, Vol. 39, 2008, pp.38–49.
[35] Villar, M.V., Water retention of two natural compacted bentonites, Clays and Clay Minerals, Vol. 55, 2007, pp.311–322.
[36] Hoffmann C., Alonso E. E. and Romero E., Hydro-mechanical behaviour of bentonite pellet mixtures. Physics and Chemistry of the Earth, Vol. 32, Issue 8–14, 2007, pp.832–849.
[37] Villar M. V., Long-Term Performance of Engineered Barrier Systems PEBS - EB Experiment, Laboratory infiltration tests report, CIEMAT Technical Report CIEMAT/ DMA/ 2G210/03/2012, 2012.
[38] Bernachy-Barbe F., Conil N., Guillot W. and Talandier J., Observed Heterogeneities after Hydration of MX-80 Bentonite under Pellet/Powder Form. Applied Clay Science, Vol. 189, Issue, February, 2020, 105542.
[39] Villar M. V. and Gomez-Espina R., Report on Thermo-Hydro-Mechanical Laboratory Tests Performed by CIEMAT on Febex Bentonite, 2004-2008, Informes Técnicos Ciemat, 1178, 2009, pp. 67.
[40] Chung C.-K., Kim J.-H., Kim J. and Kim T., Hydraulic Conductivity Variation of Coarse Fine Soil Mixture upon Mixing Ratio, Advances in Civil Engineering, Vol. 2018, 2018, pp.1-11.
[41] Villar M.V. and Lloret A., Influence of Temperature on the Hydro-Mechanical Behavior of a Compacted Bentonite, Applied Clay Science, Vol. 26, 2004, pp.337-350.
[42] Schanz T. and Al-Badran Y., Swelling Pressure Characteristics of Compacted Chinese Gaomiaozi Bentonite GMZ01, Soils and Foundations, Vol. 54, Issue 4, 2014, pp.748–759.
[43] Komine H., Simplified Evaluation for Swelling Characteristics of Bentonites, Engineering Geology, Vol. 71, Issue 3–4, 2004, pp.265–279.
[44] Molinero-Guerra A., Cui Y-J., He Y., Delage

P., Mokni N., Tang A. M., Aimedieu P., Bornert M. and Bernier F., Characterization of Water Retention, Compressibility and Swelling Properties of a Pellet/Powder Bentonite Mixture, Engineering Geology, Vol. 248, 2019, pp.14–21.

[45] Molinero-Guerra A., Aimedieu P., Bornert M., Cui Y-J., Tang A. M., Sun Z., Mokni N., Delage P. and Bernier F., Analysis of the Structural Changes of a Pellet/Powder Bentonite Mixture upon Wetting by X-Ray Computed Microtomography, Applied Clay Science, Vol. 165, Issue August, 2018, pp.164–169.

[46] García-Siñeriz J. L., Villar M. V., Rey M. and Palacios B., Engineered Barrier of Bentonite Pellets and Compacted Blocks: State after Reaching Saturation. Engineering Geology, Vol. 192, 2015, pp.33–45.

[47] Maugis P. and Imbert C., Confined Wetting of Foca Clay Powder/Pellet Mixtures: Experimentation and Numerical Modeling, Physics and Chemistry of the Earth, Vol. 32, Issue 8–14, 2007, pp.795–808.

[48] Seiphoori A., Thermo-Hydro-Mechanical Characterization and Modelling of Wyoming Granular Bentonite, Technical Report 15-05, EPFL, Lausanne, Report prepared on behalf of NAGRA, 2015.

[49] Ferrari A., Seiphoori A., Rüedi J. and Laloui L., Shot-Clay MX-80 Bentonite: An Assessment of the Hydro-Mechanical Behavior, Engineering Geology, Vol. 173, 2014, pp.10-18.

[50] Villar, M. V., Long-term Performance of Engineered Barrier Systems PEBS; Long-term THM Tests Reports: Isothermal Infiltration Tests with Materials from the HE-E, CIEMAT Technical Report, December, 2013.

[51] Molinero-Guerra A., Cui Y. J., Mokni N., Delage P., Bornert M., Aimedieu P., Tang A. M. and Bernier F., Investigation of the Hydro-Mechanical Behavior of a Pellet/Powder MX80 Bentonite Mixture using an Infiltration Column, Engineering Geology, Vol. 243, 2018, pp.18–25.

[52] Pusch R., Karlnland O. and Hokmark H., GMM – A General Microstructural Model for Qualitative and Quantitative Studies of Smectite Clays. SKB Technical Report, 90-43, Stockholm, 1990.

[53] Sinnathamby G., Korkiala-Tanttu L. and Salvador L. T., Shear Resistance of Bentonite Backfill Materials and their Interfaces under Varying Hydraulic Conditions in a Deep Rock Nuclear Waste Repository, Applied Clay Science, Vol. 104, 2015, pp.211–220.

[54] Hamamoto S., Moldrup P., Kawamoto K. and Komatsu T., Effect of Particle Size and Soil Compaction on Gas Transport Parameters in Variably Saturated, Sandy Soils. Vadose Zone Journal, Vol. 8, Issue 4, 2009, pp. 986–995.

[55] Sellin P. and Leupin O. X., The use of Clay as an Engineered Barrier in Radioactive Waste Management - A Review, Clays and Clay Minerals, Vol. 61, Issue 6, 2014, pp.477–498.

[56] Liu J. F., Skoczylas F., Talandier J. and Pu H., Dismantling of the EB Experiment: Experimental Research on the Retrieved GBM and Bentonite Blocks, Nuclear Engineering and Design, Vol. 300, Issue February, 2016, pp.297–307

[57] Villar M. V., Gutiérrez-Rodrigo V., Martín P. L., Romero F. J. and Barcala, J. M., Gas Transport in Bentonite, Technical Report, Informes Técnicos Ciemat, December, 2013.

[58] Lloret A. and Villar M. V., Advances on the Knowledge of the Thermo-Hydro-Mechanical Behavior of Heavily Compacted "FEBEX" Bentonite, Physics and Chemistry of the Earth, Vol. 32, Issue 8–14, 2007, pp.701–715.

[59] Alonso E. E., Hoffmann C. and Romero E., Pellet Mixtures in Isolation Barriers, Journal of Rock Mechanics and Geotechnical Engineering, Vol. 2, Issue 1, 2010, pp.12–31.

[60] Hamamoto S., Moldrup P., Kawamoto K., Sakaki T., Nishimura T. and Komatsu T., Pore Network Structure Linked by X-Ray CT to Particle Characteristics and Transport Parameters, Soils and Foundations, Vol. 56, Issue 4, 2016, pp.676–690.

[61] HotBENT Experiment Plan, Nagra Work Report, NAB 19-43, 2019, pp. 130.